The Journal of

Imaging Science and Technology

Reprinted from Vol. 48, 2004

IS&T

The Society for Imaging Science and Technology

http://www.imaging.org

©2004, IS&T—The Society for Imaging Science and Technology
All rights reserved. This paper, or parts thereof, may not be reproduced in any form
without the written permission of IS&T: The Society for Imaging Science and Technology,
the sole copyright owners of *The Journal of Imaging Science and Technology*.

IS&T, *Journal of Imaging Science and Technology*,
7003 Kilworth Lane, Springfield, VA 22151 USA

Pamela J. Forness
Program Manager and Managing Editor of *JIST*:
The Journal of Imaging Science and Technology
IS&T: The Society for Imaging Science and Technology
7003 Kilworth Lane
Springfield, Virginia USA 22151
Voice: 703-642-9090 extension 16
FAX: 703-642-9094
Email: pam@imaging.org <mailto:pam@imaging.org>
WEB: http://www.imaging.org

Illuminant Influence on the Reconstruction of Near-Infrared Spectra

Meritxell Vilaseca,* Jaume Pujol and Montserrat Arjona

Centre for Sensors, Instruments and Systems Development, Optics and Optometry Department, Universitat Politécnica de Catalunya, Spain

In this study we analyze the influence of the illuminant on the reconstruction of spectral reflectance curves in the near infrared region of the spectrum. We have tested several methods based on multispectral imaging that permit us to obtain the spectral reflectance of samples from measurements performed with a CCD camera. Using numerical simulation, we have analyzed the number and shape of the optimum filters that need to be used in the acquisition channels in order to obtain good spectral reconstructions under a great number of different lighting conditions. Finally, we have studied the influence of the illuminant on the quality of the reconstruction using a set of commercially available filters which are similar to the optimum filters obtained from the simulations. Our results show that the reconstruction does not depend strongly on the illuminant used. This indicates that with the same set of filters we can obtain good reconstructions for different types of illuminant.

Journal of Imaging Science and Technology 48: 111–119 (2004)

Introduction

The near-infrared region of the spectrum (NIR) has become a powerful tool for several applications in recent years. In general, the NIR spectrum of a sample has absorption peaks that correspond to the vibrational states of those molecules that are present in the material. Therefore, the spectral information included in this region can be used to identify samples. This technique is known as NIR technology[1] and is used in various different areas such as agriculture, the food industry, medical applications, the chemical industry, etc.

Conventional CCD cameras[2,3] have maximum spectral sensitivity in the visible region of the spectrum. Nevertheless, CCD cameras with an improved response in the near-infrared region are currently being manufactured and their spectral sensitivity is clearly significant when dealing with wavelengths of up to 1000 nm. Therefore, this instrumentation can be used to obtain spectral information from samples in the NIR region between 800 and 1000 nm rather than conventional spectrophotometers. The response of standard spectrophotometers is normally limited to the visible range and they must incorporate specific sensors to detect energy coming from the NIR, e.g., In GaAs, and this can significantly increase their cost.

In previous studies[4,5] we demonstrated that multispectral imaging is a good alternative methodology for reconstructing the spectral reflectance curves of samples from conventional CCD camera measurements in the NIR region of the spectrum. This technique uses different acquisition channels to obtain several images of the sample to be analyzed. Because of the different spectral responses of the channels, the images obtained contain spectral information regarding the acquired scene and it is therefore possible to calculate the spectral reflectance of the original measured sample. Several spectral reconstruction methods exist and they can be classified as interpolation methods (linear, cubic, Spline, Discrete Fourier Transform and Modified Discrete Sine Transform approximations) and estimation methods (Moore-Penrose pseudoinverse, smoothing inverse, nonlinear fittings and principal component analysis or characteristic vector analysis). For this study we used two different estimation methods: a method based on principal component analysis (PCA)[4–12] and a nonlinear estimation method (NLE).[5,13,14] These are shown to yield the best spectral reconstruction.

In order to use methods based on multispectral imaging, it is necessary to know all the spectral variables involved in the acquisition process. These spectral variables include the spectral radiance of the illuminant used to light the samples, the spectral transmittance of the filters which define each of the acquisition channels and the spectral sensitivity of the CCD camera. Once we have selected the CCD camera, we can study which type of illuminants and filters can be used in the spectrophotometric system in order to obtain the best possible reconstruction for the set of samples under consideration. Since the mathematical methods used require approximations, the factors cited (that is, the spectral distribution of the illuminant and the spectral transmittance of the filters) may yield a different reconstruction quality for the spectral reflectance curves in the NIR region. Only a few authors[15] have studied the influence of the illuminant on the measurement of color by using a multispectral imaging system, and in this case only in the visible spectrum.

In this work we study the performance of two different spectral reconstruction methods based on multispectral imaging: a principal component analysis method (PCA) and a nonlinear estimation method (NLE), under a great number of lighting conditions in the NIR region of the spectrum. The

Original manuscript received June 19, 2003

* mvilasec@oo.upc.es

©2004, IS&T—The Society for Imaging Science and Technology

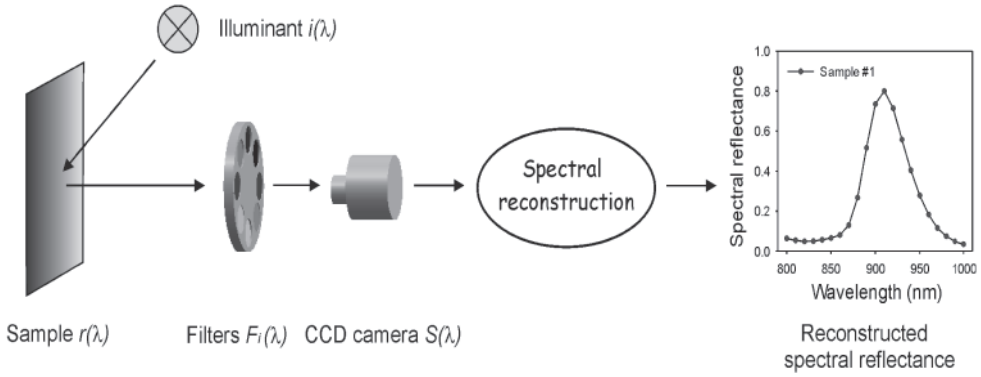

Figure 1. Schematic view of the acquisition system and the final spectral reconstruction step.

illuminants under consideration are blackbody or Planckian type emitters with color temperatures of between 1000 K and 16000 K. The following section briefly explains the most important aspects of the two methods used. Then we present our results: we perform an optimization process to determine the shape of the optimum filters that must be placed in front of the camera in order to obtain good reconstructions of the reflectance spectra of different samples for all the illuminants under consideration, and we use numerical simulation to analyze the influence of the illuminant on the quality of the reconstruction performed using commercially available filters similar to the optimum filters obtained from the simulations. Finally, we present our conclusions.

Spectral Reconstruction Methods

The reconstruction process used in methods based on multispectral imaging is summarized in Fig. 1. A multichannel image of an original object is acquired by placing a selected set of filters in front of the camera. A spectral reconstruction method is then applied in order to obtain the reconstructed spectral reflectance of the sample.

The camera responses for the different acquisition channels can be expressed in matrix notation as follows:

$$\mathbf{X} = \mathbf{Cr}, \tag{1}$$

Here, $\mathbf{X}$ is a column vector that represents the m camera's responses to a sample, $\mathbf{r}$ is a column vector (with n components) that represents the spectral reflectance of the sample, and $\mathbf{C}$ is an $(m \times n)$ matrix whose rows are the spectral sensitivities of each acquisition channel, that is,

$$C = \begin{pmatrix} i(\lambda_1)F_1(\lambda_1)S(\lambda_1)\ldots i(\lambda_n)F_1(\lambda_n)S(\lambda_n) \\ \vdots \qquad\qquad\qquad\qquad \vdots \\ i(\lambda_1)F_1(\lambda_1)S(\lambda_1)\ldots i(\lambda_n)F_1(\lambda_n)S(\lambda_n) \end{pmatrix}, \tag{2}$$

where $i(\lambda_l)$ is the spectral radiance of the illuminant, $F_i(\lambda_l)$ the spectral transmittance of the filters placed between the camera and the sample, and $S(\lambda_l)$ the spectral sensitivity of the CCD camera.

In this study we analyze the performance of a PCA and an NLE spectral reconstruction method. In order to use these methods it is necessary to know a set of spectral reflectances similar to the curves that we intend to reconstruct. The set of p known spectral reflectances is represented by an $(n \times p)$ matrix called the original data matrix ($\mathbf{O}_r$).

The PCA method associates the matrix $\mathbf{O}_r$ to an n-dimensional vector space and its characteristic vectors can be calculated. The method allows us to approximate each of the curves that belong to the original data matrix or spectra similar to them by performing a linear combination of the largest calculated characteristic vectors,

$$\mathbf{r_{rec}} = \mathbf{r_M} + \alpha\mathbf{v_{r1}} + \beta\mathbf{v_{r1}} + \ldots + \xi\mathbf{v_{rq}},\ q < n, \tag{3}$$

where $\mathbf{r_{rec}}$ is the reconstructed spectral reflectance, $\mathbf{r_M}$ is the mean spectral reflectance of the curves belonging to $\mathbf{O_r}$, $\mathbf{v_{r1}}$, $\mathbf{v_{r2}}$,...,$\mathbf{v_{rq}}$ are the characteristic vectors and α, β,.., ξ are scalar coefficients.

The scalar coefficients can be determined experimentally by relating the camera responses for each sample to the characteristic vectors, that is, by combining Eqs. (1) and (3):

$$\mathbf{X} = \mathrm{C}\mathbf{r} \approx \mathbf{Cr_M} + \alpha\mathbf{Cv_{r1}} + \beta\mathbf{Cv_{r1}} + \ldots + \xi\mathbf{Cv_{rq}},\ q < n. \tag{4}$$

The NLE method used is a modification of the conventional Wiener estimation method.[15,16] In the case of the Wiener estimation, we assume that a matrix, $\mathbf{D}$, exists and that it provides the spectral reflectances of the samples belonging to the matrix $\mathbf{O_r}$ from the camera responses. In other words:

$$\mathbf{O_r} = \mathbf{DX_{Or}}, \tag{5}$$

where $\mathbf{X_{Or}}$ is an $(m \times p)$ matrix whose columns are the camera responses for each of the known samples for the different existing channels,

$$\mathbf{X_{Or}} = \begin{pmatrix} X_{1,1} & X_{1,2} & \ldots & X_{1,p} \\ X_{2,1} & X_{2,2} & & \\ \vdots & \vdots & & \vdots \\ X_{m,1} & X_{m,2} & \ldots & X_{m,p} \end{pmatrix} = \mathbf{CO_r}. \tag{6}$$

Combining Eqs. (5) and (6), we obtain:

$$\mathbf{O_r} = \mathbf{DCO_r} \tag{7}$$

Inverting Eq. (7) by using the pseudoinverse technique,[15-19] which searches for a least-squares solution and gives the least-norm solution, we obtain a matrix, $\mathbf{D}$, which minimizes the distance between the known and the estimated spectral reflectances:

$$\mathbf{D} = \mathbf{O_r X_{Or}^T (X_{Or} X_{Or}^T)^{-1}} = \mathbf{O_r O_r^T C^T (C O_r O_r^T C^T)^{-1}}. \quad (8)$$

We assume that the reflectance spectra to be reconstructed are a linear combination of the known spectral curves, that is, that the curves belonging to $\mathbf{O_r}$ are a good representation of all the spectra. This can be stated as follows:

$$\mathbf{r} \approx \mathbf{O_r}\alpha, \quad (9)$$

where α is a column vector whose components are the coefficients of the linear combination. Therefore, matrix $\mathbf{D}$ is valid for the reconstruction of any curve $\mathbf{r}$:

$$\mathbf{r_{rec}} = \mathbf{DX} = \mathbf{DCr} \approx \mathbf{DCO_r}\alpha. \quad (10)$$

In this method we have used a linear transformation to relate the reflectance spectra to the camera responses (Eqs. (5) and (6)). By extension, we can also apply a nonlinear transformation. Instead of using the matrix $\mathbf{X_{Or}}$ we can consider a matrix $\mathbf{X_{NL}}$, whose columns are a second or higher order polynomial that represent the camera responses. We can then calculate another matrix, $\mathbf{D_{NL}}$, which relates the polynomial data to the spectral reflectances. Using a complete second order polynomial and three available channels, matrix $\mathbf{X_{NL}}$ would be:

$$\mathbf{X_{NL}} = \begin{pmatrix} 1 & 1 & \dots & 1 \\ X_{1,1} & X_{1,2} & \dots & X_{1,p} \\ X_{2,1} & X_{2,2} & \dots & X_{2,p} \\ X_{3,1} & X_{3,2} & \dots & X_{3,p} \\ X_{1,1}^2 & X_{1,2}^2 & \dots & X_{1,p}^2 \\ X_{2,1}^2 & X_{2,2}^2 & \dots & X_{2,p}^2 \\ X_{3,1}^2 & X_{3,2}^2 & \dots & X_{3,p}^2 \\ X_{1,1}X_{2,1} & X_{1,2}X_{2,2} & \dots & X_{1,p}X_{2,p} \\ X_{1,1}X_{3,1} & X_{1,2}X_{3,2} & \dots & X_{1,p}X_{3,p} \\ X_{2,1}X_{3,1} & X_{2,2}X_{3,2} & \dots & X_{2,p}X_{3,p} \end{pmatrix}^T. \quad (11)$$

Matrix $\mathbf{D_{NL}}$ is calculated as in the Wiener estimation:

$$\mathbf{D_{NL}} = \mathbf{O_r X_{NL}^T (X_{NL} X_{NL}^T)^{-1}}. \quad (12)$$

We can use polynomials of any order or shape. In practice, this is limited by the precision we require and the computational costs. The intersection between channels is often small and therefore, an increase in the order of the polynomial may not result in a significant improvement of the reconstructions. In this work we use the proposed NLE method with a complete second order polynomial.

Finally, in order to evaluate the quality of the reconstruction of the analyzed spectra we use two different parameters:

Percentage of reconstruction:

$$P_{rec} = \left[1 - \frac{\sum_{\lambda_{\min}}^{\lambda_{\max}} (r - r_{rec})^2}{\sum_{\lambda_{\min}}^{\lambda_{\max}} (r)^2}\right] \times 100, \quad (13)$$

and Root Mean Square Error:

$$RMSE = \left[\frac{1}{N_\lambda} \sum_{\lambda_{\min}}^{\lambda_{\max}} (r - r_{rec})^2\right]^{1/2}. \quad (14)$$

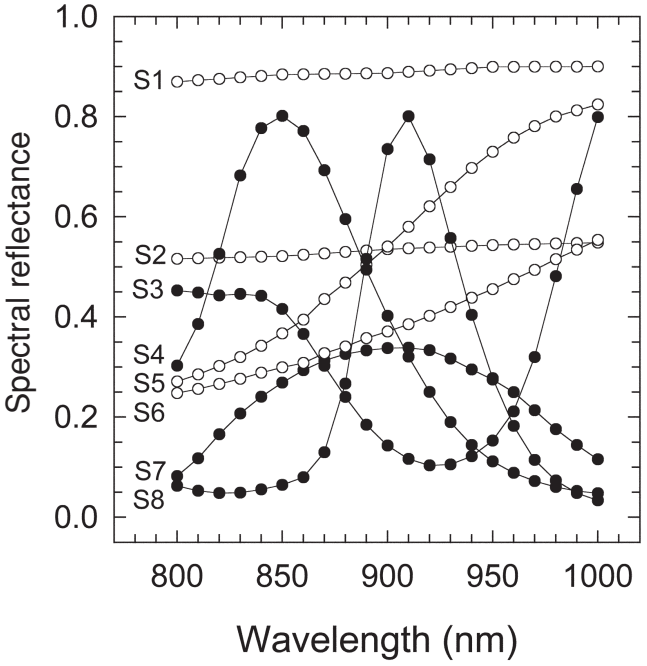

Figure 2. Spectral reflectance curves of 8 representative samples belonging to matrix $\mathbf{O_r}$.

where each r represents an experimental component of the original reflectance curves, each r_{rec} is a reconstructed value, and N_λ is the number of wavelengths at which measurements were made.

Although in multispectral imaging *RMSE* is the most commonly used parameter, we have also used the percentage of reconstruction because it provides an intuitive idea of the quality of the reconstruction since its maximum possible value is 100. Both parameters are very sensitive to variations in the reconstructions. Good reconstructions are achieved if P_{rec} is greater than 99.9% and *RMSE* is smaller than 0.01.[4,5] Depending on the case, slightly different values can lead to considerable differences between the original and the reconstructed spectra.

Results

Data

In this work we have mainly analyzed the influence the illuminant has on the reconstruction of the spectral reflectance in the NIR region of the spectrum by using numerical simulation. In order to perform the simulations we considered an original data matrix, $\mathbf{O_r}$, composed of 30 spectral reflectance curves that correspond to textile samples (Fig. 2). As we considered the spectral data between 800 and 1000 nm in 10 nm steps, each curve was made up of 21 components. The CCD camera used in the acquisition process was a JAI CV-M10 progressive scan camera, whose spectral sensitivity was measured experimentally and is shown in Fig. 3.

The different illuminants analyzed were blackbody or Planckian type (specifically graybody) radiators with the following color temperatures: 1000, 1500, 1800, 1850, 1900, 2000, 2852, 3371, 4000, 5000, 6000, 7000, 8000, 9000, 12000, 13000, 14000 and 16000 K (Figs. 4(a) and 4(b)). The use of this range of color temperatures is justified by the clearly different spectral profiles of the illuminants in the region studied. Color temperatures of 2852 and 3371 K correspond to commercially available sources, commonly

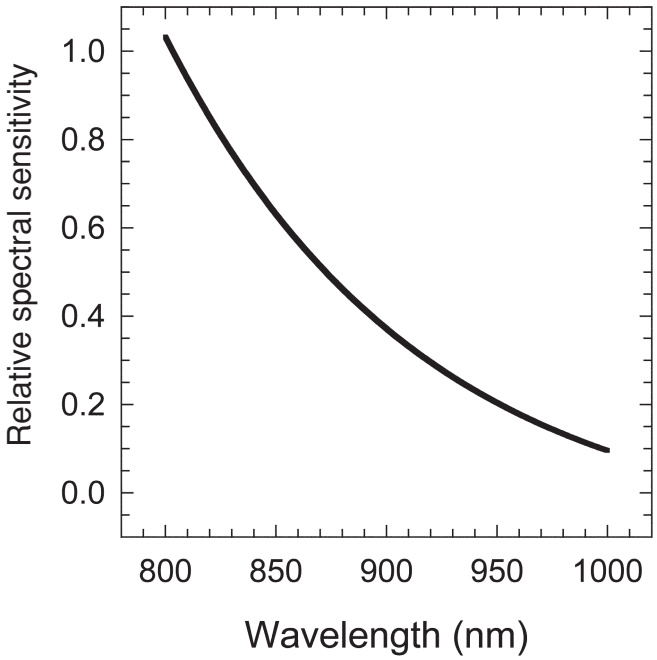

Figure 3. Relative spectral sensitivity of the JAI CV-M10 camera.

used in spectrophotometric devices. The total emission of the illuminants was normalized to a specific radiance (10^5 W/sr*m^2) in order to obtain simulated lamps with the same radiant flux.

Reconstructions with Simulated Gaussian Filters

In this section we perform a numerical simulation in order to analyze the shape of the optimum filters that must be placed in front of the camera to obtain the best reconstruction results under the influence of all the lighting conditions under consideration. In previous work,[4,5] we demonstrated that filters with Gaussian transmittance profiles give rise to good reconstructions of spectral reflectance curves in the NIR region. Specifically, we demonstrated that five and three equally-spaced Gaussian filters were enough to achieve good results in the case of the PCA and NLE methods, respectively. Gaussian filters are useful because they have simple transmittance profiles and therefore they can be replaced experimentally by commercially available filters. The transmittance of each Gaussian filter can be expressed as follows:

$$T(\lambda) = T_{MAX} \exp\left[-4 \ln 2 \left(\frac{\lambda - \lambda_0}{FWHM}\right)^2\right], \quad (15)$$

where T_{MAX} is the maximum transmittance, λ_0 is the wavelength corresponding to the maximum transmittance and FWHM is the full width-half maximum of the Gaussian filter.

T_{MAX} is considered to be unity in this study, and λ_0 has fixed values since the filters are equally spaced within the NIR region. The spectral bandwidth of the filters (*FWHM*) is considered to be the optimization parameter.

In the simulation, the filters with optimum *FWHM* were determined by searching for the minimum mean *RMSE* of the curves belonging to the matrix $\mathbf{O}_r$, using the two

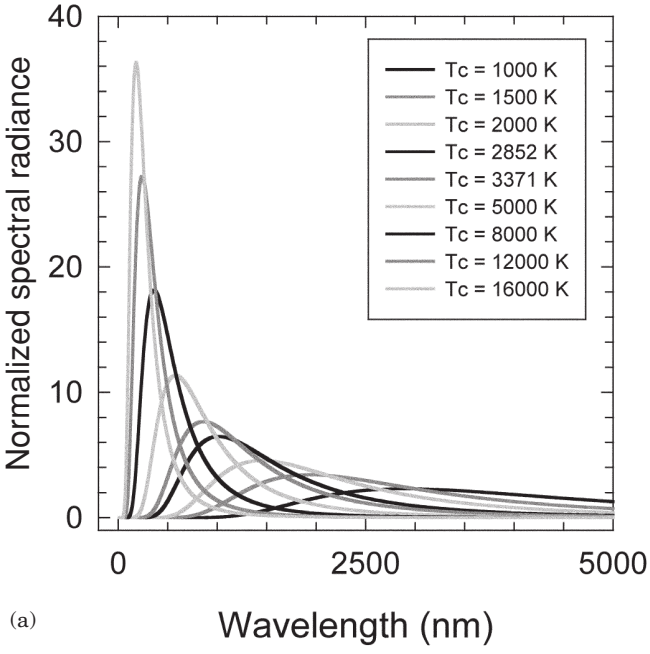

(a)

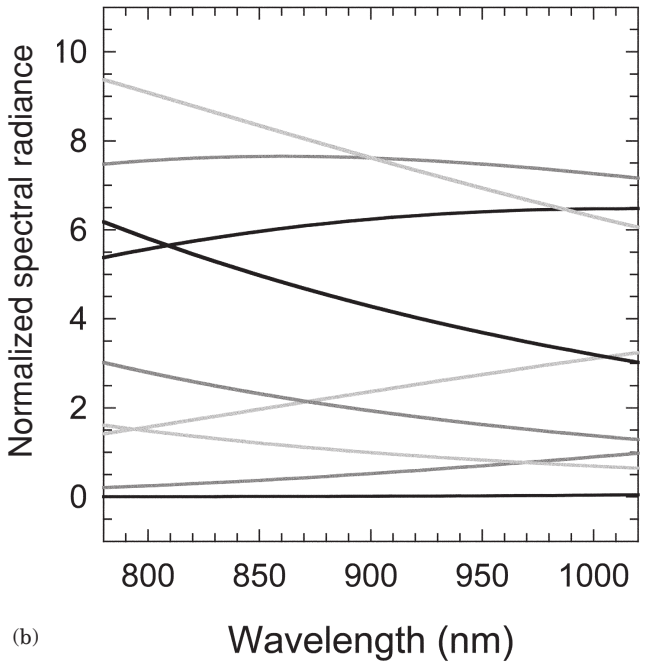

(b)

Figure 4. Spectral radiance of the illuminants analyzed normalized to 10^5 W/sr*m^2 between 0 and 5000 nm (a) and between 800 and 1000 nm (b).

proposed reconstruction methods. Tables I, II and III show the optimization results for the PCA method with five filters and the NLE method with three and five filters, using the illuminants of different color temperatures. These tables include the optimum parameter *FWHM*, and mean P_{rec} and *RMSE* values for all the simulated cases. Figure 5 represents the evolution of *FWHM* with color temperature.

It can be seen that the optimum *FWHM* is different for each method and its evolution with color temperature varies depending on the case under consideration. In general, at

TABLE I. Optimum *FWHM* of the filters, Mean P_{rec} and *RMSE* values obtained using the PCA method, five simulated Gaussian filters and the illuminants with different color temperatures.

Tc (K)	*FWHM* (nm)	Mean P_{rec}	Mean (*RMSE**100)
1000	122	99.996	0.170
1500	97	99.996	0.183
1800	87	99.995	0.191
1850	85	99.995	0.193
1900	82	99.995	0.194
2000	80	99.995	0.197
2852	66	99.995	0.215
3371	61	99.994	0.223
4000	59	99.994	0.229
5000	57	99.994	0.237
6000	57	99.994	0.242
7000	54	99.994	0.245
8000	54	99.993	0.248
9000	54	99.993	0.250
12000	54	99.993	0.253
13000	54	99.993	0.254
14000	52	99.993	0.255
16000	52	99.993	0.256

TABLE II. Optimum *FWHM* of the filters, Mean P_{rec} and *RMSE* values obtained using the NLE method, three simulated Gaussian filters and the illuminants with different color temperatures.

Tc (K)	*FWHM* (nm)	Mean P_{rec}	Mean (*RMSE**100)
1000	28	99.941	0.607
1500	31	99.942	0.603
1800	31	99.942	0.602
1850	31	99.943	0.602
1900	31	99.943	0.602
2000	31	99.943	0.601
2852	31	99.943	0.600
3371	31	99.943	0.600
4000	31	99.944	0.600
5000	31	99.944	0.600
6000	31	99.944	0.600
7000	31	99.944	0.600
8000	31	99.944	0.600
9000	28	99.944	0.600
12000	28	99.945	0.600
13000	28	99.945	0.600
14000	28	99.945	0.600
16000	28	99.945	0.600

TABLE III. Optimum *FWHM* of the filters, Mean P_{rec} and *RMSE* values obtained using the NLE method, five simulated Gaussian filters and the illuminants with different color temperatures.

Tc (K)	*FWHM* (nm)	Mean P_{rec}	Mean (*RMSE**100)
1000	66	100	0.032
1500	92	100	0.014
1800	38	100	0.014
1850	89	100	0.014
1900	38	100	0.013
2000	82	100	0.015
2852	80	100	0.016
3371	78	100	0.016
4000	80	100	0.016
5000	103	100	0.016
6000	103	100	0.017
7000	97	100	0.016
8000	99	100	0.016
9000	97	100	0.016
12000	101	100	0.016
13000	103	100	0.016
14000	99	100	0.016
16000	101	100	0.016

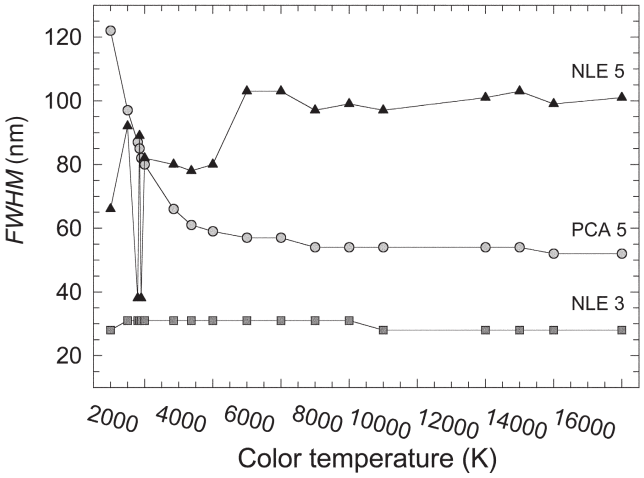

Figure 5. Evolution of the parameter *FWHM* of the filters according to the color temperature of the illuminant used (PCA 5: PCA method and 5 filters, NLE 3/5: NLE method and 3 or 5 filters, respectively).

low color temperatures, each method analyzed behaves differently. However, for color temperatures above 5000 K or 6000 K the optimum spectral bandwidth stabilizes in all the cases studied. PCA and NLE methods are techniques which use camera responses to reconstruct the spectral reflectance of samples. In order to obtain similar results from the optimization process of the filters for different color temperatures, it is necessary to have similar values of the camera responses for the samples analyzed under the influence of the different illuminants. The camera responses of any sample for all the acquisition channels can be expressed by Eq. (1), that is:

$$\mathbf{X} = \mathbf{Cr}, \tag{16}$$

The explicit form of this expression for each acquisition channel is:

$$X_i = \sum_{\lambda} i(\lambda)S(\lambda)r(\lambda). \tag{17}$$

Thus, in order to have similar camera responses for each channel, and therefore obtain similar optimum *FWHM* values in the optimizations for different analyzed illuminants, the spectral products of the samples ($i_\lambda S_\lambda r_\lambda$) must be almost the same. Figures 6(a) and 6(b) show these terms for two particular samples belonging to the matrix $\mathbf{O_r}$ (S2 and S3). In both figures it can be seen that the spectral curves are more similar at longer wavelengths (particularly above 900 nm) than in other parts of the spectrum. This is due to the influence of the spectral sensitivity of the camera, whose profile decreases in the region studied. It can be seen that for color temperatures above 5000 K, the spectral products have profiles with a large similarity across all the wavelengths. This can be explained by the spectral

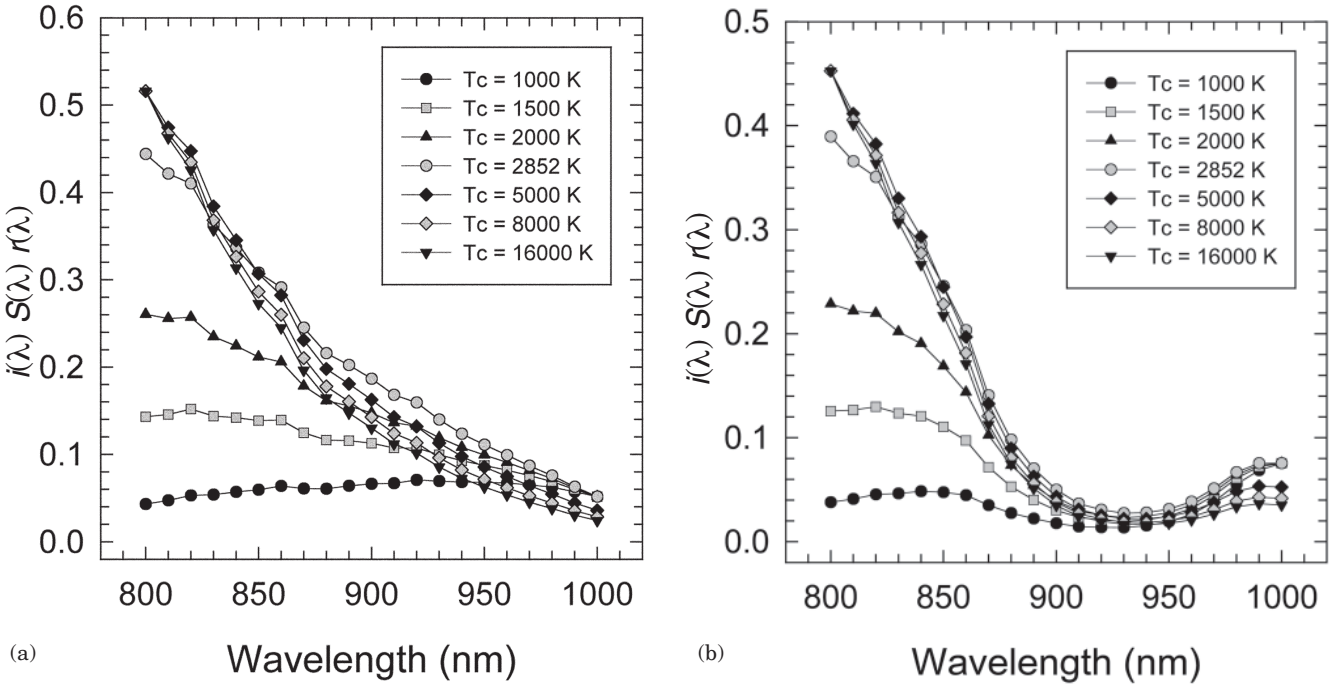

Figure 6. Spectral curves corresponding to the product $i(\lambda)\ S(\lambda)\ r(\lambda)$ of sample S2 (a) and S3 (b), both belonging to $\mathbf{O}_r$ ($i(\lambda)$: spectral radiance of the illuminant, $S(\lambda)$: spectral sensitivity of the CCD camera, and $r(\lambda)$: spectral reflectance of the samples).

emission of the illuminants in the NIR region: because the illuminants with large color temperatures have maximum emission peaks located at short wavelengths, they have a similar decreasing spectral distribution between 800 and 1000 nm. These resemblances are translated to similar spectral bandwidths of the optimum filters obtained and therefore explain the stability of the results at these color temperatures in all the cases analyzed. Below 5000 K, the spectral distribution of the illuminants in the NIR region changes much more, depending on the color temperature. In the case of the PCA method, a decrease in the color temperature produces an increase in optimum *FWHM*. In the case of the NLE method, the optimization results depend on the number of filters used to perform the reconstruction. Using three filters, the *FWHM* values are largely constant, but with five filters, the results show remarkable oscillations. The NLE method uses the pseudoinverse technique which computes the pseudoinverse of a non-square matrix. This technique involves the calculation of the inverse of a square matrix with singularities (Eq. (12)). Therefore, the results obtained are very sensitive to variations in input data and they may present oscillations. In the three-filter case, the matrix $\mathbf{X}_{\mathbf{NL}}$ has lower dimensions than in the case of five filters. Therefore, the pseudoinverse procedure does not involve as many singularities as in the five-filter case and it is more stable.

Figures 7(a) and 7(b) show the evolution of the equivalent P_{rec} and *RMSE* with color temperature. In the case of the PCA method, *RMSE* increases with color temperature. In the case of the NLE method, the *RMSE* values decrease but they are almost constant for all the lighting conditions analyzed. However, in all the reconstructions performed, $P_{rec} \geq 99.9\%$ and $(RMSE \times 100) \leq 1$. In previous work,[4,5] we demonstrated that these values guarantee acceptable reconstructions in the NIR region of the spectrum for any sample.

The use of filters with non-optimal spectral characteristics can yield worse reconstruction parameters. Depending on the sample, a greater difference than 0.01 in *RMSE* (or equivalently a P_{rec} smaller than 99.9%) can imply a considerable dissimilarity between the original and the reconstructed reflectance curves. The values of both parameters are very sensitive to variations in the reconstructions. For instance, if an original and a reconstructed curve are very similar in almost all the wavelengths except in some of them where a local peak has appeared in the reconstructed spectrum (which does not exist in the original), the parameters can be slightly modified while the spectra are very different.

Reconstructions with Real Filters

In this section we analyze the quality of the reconstructions of the samples using real commercial filters, under the influence of all the different lighting conditions considered. In the previous section we presented optimizations performed with simulated Gaussian filters. We saw that in general the optimum spectral bandwidth of the filters depends on the illuminant under consideration and the methods used. Taking into account that incandescent or halogen lamps (which are used in many spectrophotometric devices) have color temperatures in the 2800 – 3100 K range, we can consider as optimum the results obtained using illuminants with color temperatures of 2852 K and 3371 K. In the case of the PCA method, the optimum spectral bandwidth of the filters for these two illuminants is 66 nm and 78 nm, respectively. In the case of the NLE method, the *FWHM* values are 31 nm using three filters, and 80 nm and 78 nm using five filters. In conventional commercial catalogues published by different manufacturers we can find common interference filters with the following spectral bandwidths (*FWHM*): 1.5, 3, 10, 25, 40 and 70 nm. The most similar, in almost all the cases considered (except for the NLE method with three filters), to those obtained in the simulation process are the filters with a *FWHM* of 70 nm. We acquired five filters with these spectral features (Thermo Corion interference filters) equally spaced within

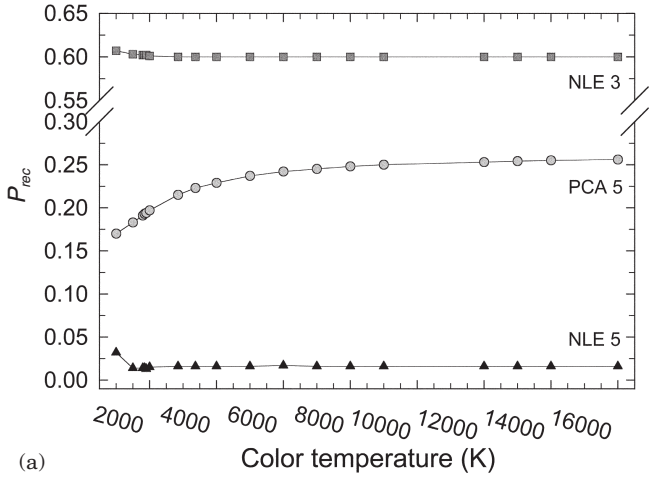

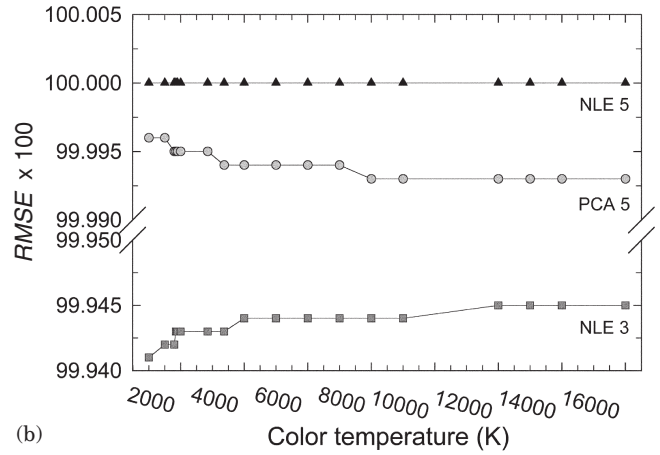

Figure 7. Evolution of the parameter P_{rec} (a) and *RMSE* (b) according to the color temperature of the illuminant, using the optimum Gaussian filters (PCA 5: PCA method and 5 filters, NLE 3/5: NLE method and 3 or 5 filters, respectively).

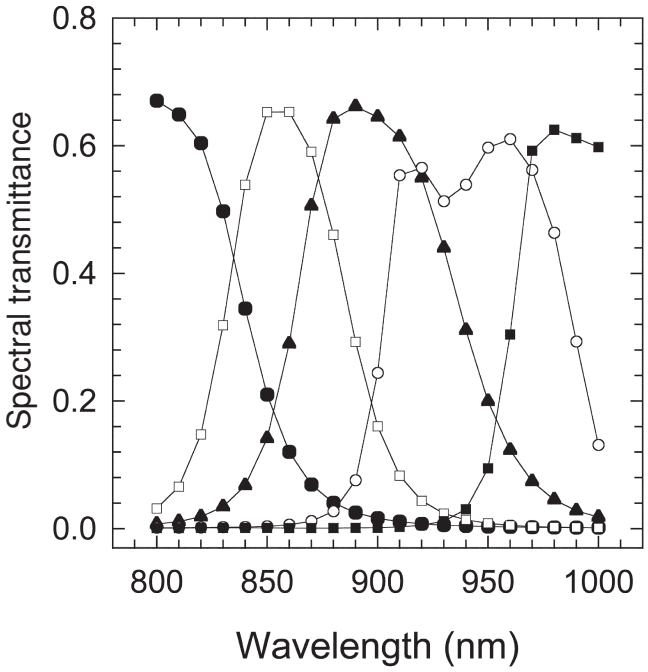

Figure 8. Spectral transmittance of the real interference filters.

the range analyzed, that is, the NIR region (Fig. 8). It was then possible to assess the reconstructions using these filters under the influence of the different illuminants. In the case of the NLE method with three filters, we considered those centered at the wavelengths of 850, 900 and 950 nm.

Table IV presents the reconstruction results obtained using the PCA method for all the illuminants and the results for the NLE method with three and five filters are exposed in Tables V and VI, respectively. Figures 9(a) and 9(b) show how the P_{rec} and *RMSE* change with the color temperature.

The results are quite similar to those obtained using the optimum Gaussian filters. While in the case of the PCA method the *RMSE* increases when the color temperature is increased, in the NLE method the results are almost constant for the different lighting conditions analyzed.

In general, the results are worse since the real filters actually used do not have exactly the same spectral profile as the optimum Gaussian filters obtained in the previous section. Also, for all the reconstructions performed, $P_{rec} \geq 99.9\%$ and $(RMSE \times 100) \leq 1$. Therefore, the set of commercial filters analyzed can be used to obtain spectral reflectance curves under the influence of all the illuminants analyzed and might be useful for an experimental spectrophotometric system. For the experimental implementation is interesting to analyze the effect of the noise on the reconstruction parameters. The different possible sources of noise or experimental errors that can be present in a reconstruction system[20] (random noise, quantization noise, spectral reflectance measurement errors, errors of the geometry or position of the elements present in the experiment, etc.) can be considered together in order to simplify the treatment in our simulations, adding or subtracting a specific quantity to the simulated camera responses for each channel and sample. In the analyzed cases, the noise level must be smaller than 1% in order to achieve acceptable results, that is, similar values to the simulations, but it will be studied in detail in further work.

Conclusions

In this work, we have mainly studied the influence of the illuminant on the reconstruction of NIR spectra using multispectral imaging methods. We have used a method based on principal component analysis (PCA) and a nonlinear estimation method (NLE) which uses a complete second-order polynomial, to obtain the reflectance spectra in the NIR region by use of CCD camera measurements, under different lighting conditions. The illuminants analyzed were graybody radiators with color temperatures of between 1000 K and 16000 K, all with the same radiant flux. In the first part of the study, we used five equally-spaced Gaussian filters in the case of the PCA method, and three and five filters for the NLE method, in order to reconstruct the spectral reflectance curves of 30 textile samples. We determined the optimum spectral bandwidth (*FWHM*) of the filters in order to obtain the best possible reconstruction for each case analyzed, that is, for each illuminant and method tested. It can be seen that the optimum *FWHM* depends on the reconstruction method and the illuminant used but there is a stabilization of the results for color temperatures

TABLE IV. Mean P_{rec} and *RMSE* values obtained using the PCA method, the five real interference filters and the illuminants with different color temperatures.

Tc (K)	Mean P_{rec}	Mean (*RMSE**100)
1000	99.995	0.184
1500	99.994	0.210
1800	99.992	0.227
1850	99.992	0.230
1900	99.992	0.232
2000	99.992	0.238
2852	99.988	0.280
3371	99.985	0.302
4000	99.983	0.324
5000	99.979	0.351
6000	99.977	0.371
7000	99.974	0.387
8000	99.973	0.399
9000	99.971	0.409
12000	99.968	0.428
13000	99.967	0.433
14000	99.967	0.437
16000	99.966	0.443

TABLE V. Mean P_{rec} and RMSE values obtained using the NLE method, three real interference filters and the illuminants with different color temperatures.

Tc (K)	Mean P_{rec}	Mean (*RMSE**100)
1000	99.886	0.782
1500	99.887	0.764
1800	99.885	0.766
1850	99.885	0.767
1900	99.885	0.767
2000	99.884	0.769
2852	99.880	0.782
3371	99.877	0.789
4000	99.875	0.797
5000	99.873	0.805
6000	99.871	0.811
7000	99.870	0.815
8000	99.869	0.818
9000	99.868	0.821
12000	99.867	0.826
13000	99.866	0.827
14000	99.866	0.828
16000	99.866	0.829

TABLE VI. Mean P_{rec} and *RMSE* values obtained using the NLE method, the five real interference filters and the illuminants with different color temperatures.

Tc (K)	Mean P_{rec}	Mean (*RMSE**100)
1000	100	0.044
1500	100	0.015
1800	100	0.015
1850	100	0.015
1900	100	0.016
2000	100	0.016
2852	100	0.016
3371	100	0.017
4000	100	0.017
5000	100	0.017
6000	100	0.017
7000	100	0.017
8000	100	0.017
9000	100	0.017
12000	100	0.018
13000	100	0.018
14000	100	0.018
16000	100	0.018

above 5000 or 6000 K. Based on the results obtained, we acquired a set of commercially available filters (Thermo Corion interference filters) and analyzed the quality of the reconstruction achieved using them under the influence of the different illuminants considered. Our results show that $P_{rec} \geq 99.9$ % and $RMSE \leq 0.01$ in all the cases analyzed. This indicates that with the same set of filters we can obtain good reconstructions of the spectral reflectance curves in the NIR region for all the samples considered, using any of the tested illuminants. Particularly, since incandescent or halogen lamps usually have color temperatures between 2800 and 3100 K, it would be possible to make a real instrument using any of them.

Acknowledgment. This research was supported by the Spanish Ministry for Science and Technology (Ministerio

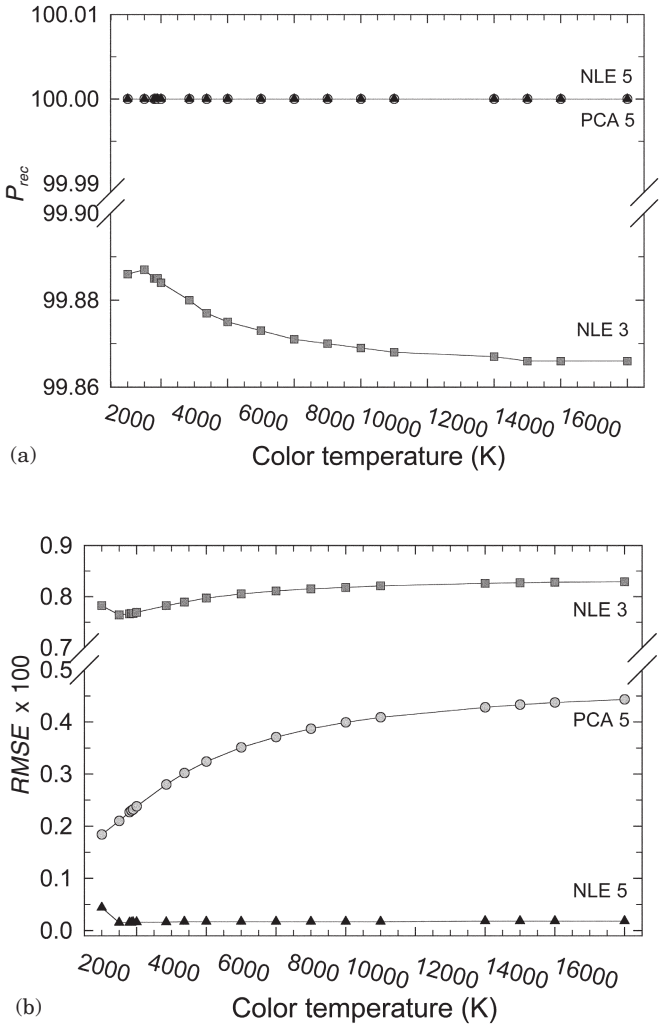

Figure 9. Evolution of the parameter P_{rec} (a) and *RMSE* (b) according to the color temperature of the illuminant, using the real interference filters (PCA 5: PCA method and 5 filters, NLE 3/5: NLE method and 3 or 5 filters, respectively).

de Ciencia y Tecnología) by means of the grant number DPI2002-00118. M. Vilaseca would like to thank the Generalitat (government) of Catalonia for the Ph.D. grant that she received.

References

1. J. M. Pope, NIR gains continue in on-line process applications, *Chiltons I&CS* **67,** 45 (1994).
2. G. C. Holst, *CCD Arrays, Cameras and Displays,* SPIE Press, Bellingham, WA, 1998.
3. G. C. Holst, *Handbook of Optics III*, McGraw-Hill, New York, 2001, p. 41.
4. M. Vilaseca, J. Pujol and M. Arjona, Spectral-reflectance reconstruction in the near-infrared region by use of conventional charge-couple-device camera measurements, *Appl. Opt.* **10,** 1788 (2003).
5. M. Vilaseca, J. Pujol and M. Arjona, NIR spectrophotometric system based on a conventional CCD camera, *Proc. SPIE* **5011,** 222 (2003).
6. J. L. Simonds, Application of characteristic vector analysis to photographic and optical response data, *J. Opt. Soc. Amer.* **53,** 968 (1963).
7. Y. Chang, P. Liang and S. Hackwood, Unified study of color sampling, *Appl. Opt.* **28,** 809 (1989).
8. M. J. Vrhel, R. Gershon and L. S. Iwan, Measurement and analysis of object reflectance spectra, *Color Res. Appl.* **19,** 4 (1994).
9. S. Tominaga, Multichannel vision system for estimating surface and illumination functions, *J. Opt. Soc. Amer. A* **13,** 2163 (1989).
10. F. Imai and R. S. Berns, Comparative analysis of spectral reflectance reconstruction in various spaces using a trichromatic camera system, *J. Imaging Sci. Technol.* **44,** 280 (2000).
11. J. Y. Hardeberg, F. Schmitt and H. Brettel, Multispectral image capture using a tunable filter, *Proc. SPIE* **3963,** 77 (2000).
12. I. T. Jolliffe, *Principal Component Analysis*, Springer-Verlag, New York, 1986.
13. P. G. Herzog, D. Knipp, H. Stiebig, and F. König, Colorimetric characterization of novel multiple-channel sensors for imaging and metrology, *J. Electron. Imaging* **8,** 342 (1999).
14. G. Hong, M. R. Luo and P.A. Rhodes, A study of digital camera colorimetric characterization based on polynomial modeling, *Color Res. Appl.* **26,** 76 (2001).
15. J. Y. Hardeberg, F. Schmitt, H. Brettel, J-P. Crettez and H. Maître, *Colour Imaging: Vision and Technology*, John Wiley and Sons, Chichester, UK, 1999, p. 145.
16. M. Vilaseca, J. Pujol, M. Arjona and F. Martínez-Verdú, Illuminant influence on the reconstruction of NIR spectra, in *Proc. of IS&T's PICS Conference*, IS&T, Springfield, VA 2003, pp. 536-541.
17. F. König and W. Praefcke, The practice of multispectral image acquisition, *Proc. SPIE* **3409,** 34 (1998).
18. D. Hanselman and B. Littlefield, *Matlab 5. A Comprehensive Tutorial and Reference*, Prentice Hall, New Jersey, 1998.
19. A. Albert, *Regression and the Moore-Penrose Pseudoinverse*, Academic Press, New York, 1972.
20. P. M. Hubel, D. Sherman and J. E. Farrel, A comparison of methods of sensor spectral sensitivity estimation, in *Proc. IS&T/SID's 2nd Color Imaging Conference: Color Science, Systems and Applications*, IS&T, Springfield, VA, 1994, pp. 45-48.